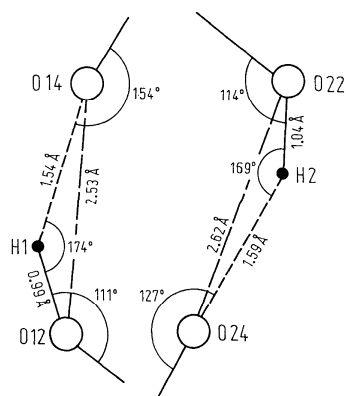
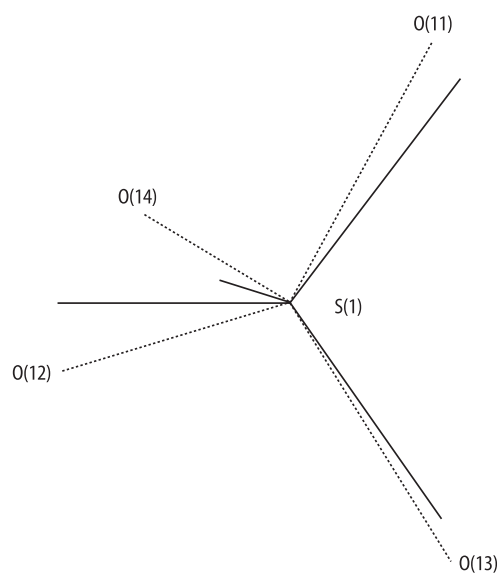


**Fig. 40A-2-001.**  $\text{RbHSO}_4$ . Structure of phase I [75Ash]. Projection on (010). See also Table 40A-2-001 and Table 40A-2-003.



**Fig. 40A-2-002.**  $\text{RbHSO}_4$ . Structure of phase I [75Ash]. Geometries of the two hydrogen bonds obtained by neutron diffraction at 23 °C. See also Table 40A-2-003.



**Fig. 40A-2-003.**  $\text{RbHSO}_4$ . Structure of phase I [95Ito]. Two orientational arrangements of disordered  $\text{SO}_4(1)$  ion.

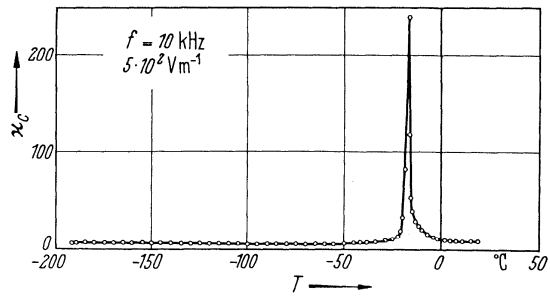


Fig. 40A-2-004.  $\text{RbHSO}_4$ .  $\kappa_c$  vs.  $T$  [60Pep].

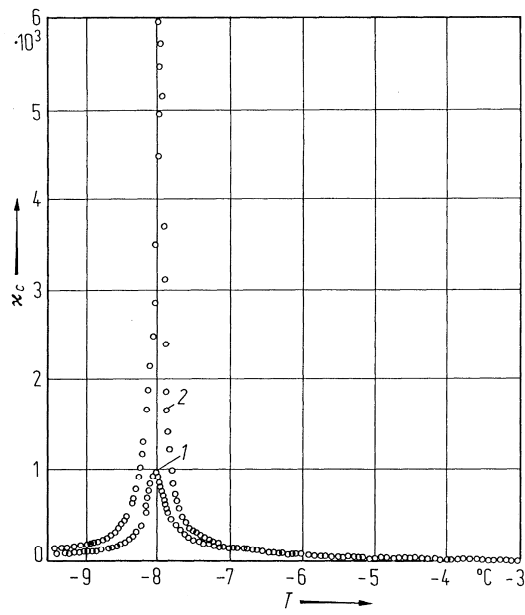
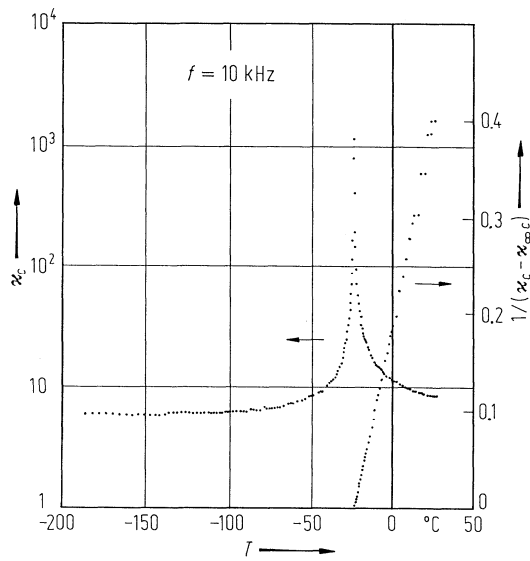
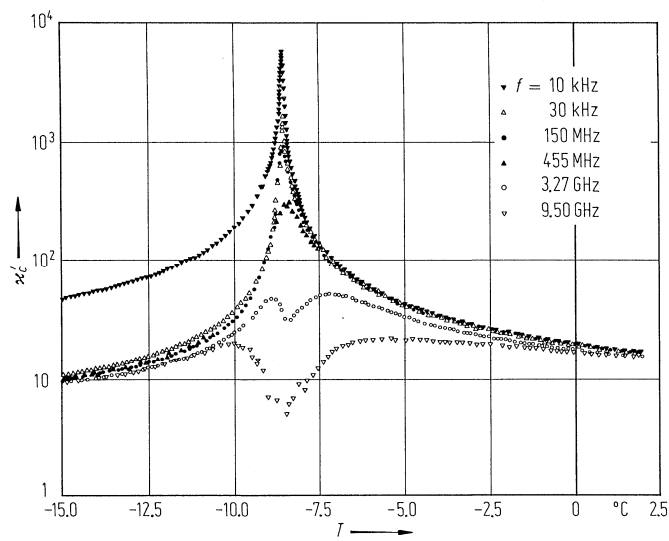


Fig. 40A-2-005.  $\text{RbHSO}_4$ .  $\kappa_c$  vs.  $T$  [77Kaj]. Curve 1: as grown, 2: annealed at  $180^{\circ}\text{C}$  for 43 h.  $\kappa_c$  at  $f = 10 \text{ kHz}$ .



**Fig. 40A-2-006.**  $\text{RbDSO}_4$ .  $\kappa_c$ ,  $1/(\kappa_c - \kappa_{\infty c})$  vs.  $T$  [79Ich].  $\kappa_{\infty c}$ : temperature independent term of the dielectric constant along the ferroelectric  $c$  axis.



**Fig. 40A-2-007.**  $\text{RbHSO}_4$ .  $\kappa'_c$  vs.  $T$  [80Oza]. Parameter:  $f$ . Up to 9.50 GHz.

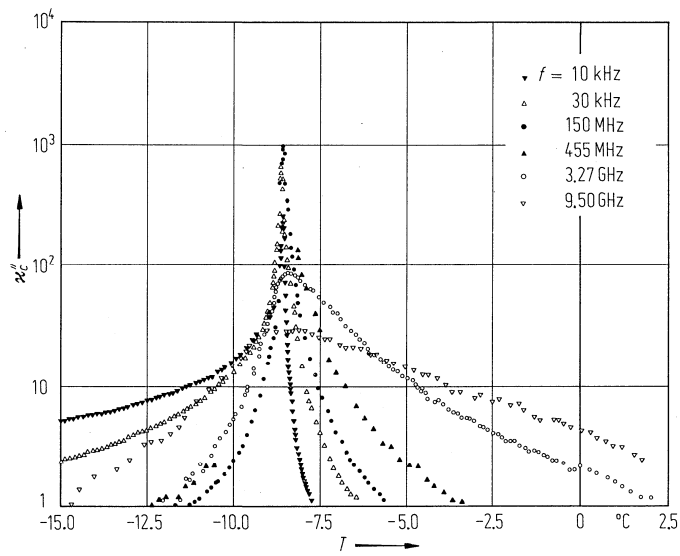


**Fig. 40A-2-008.**  $\text{RbHSO}_4$ .  $\kappa''_c$  vs.  $T$  [80Oza]. Parameter:  $f$ . Up to 9.50 GHz.

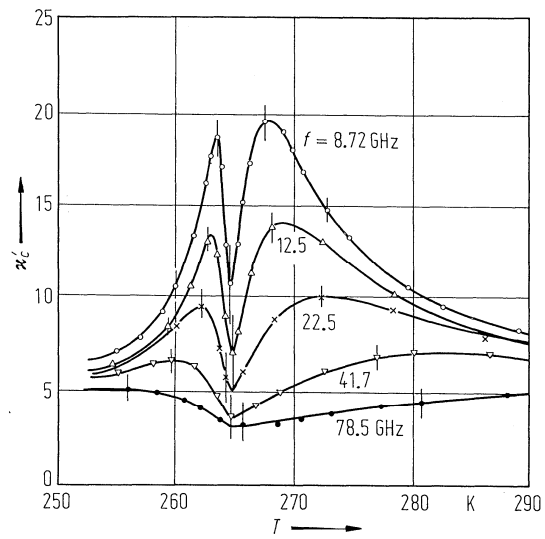


**Fig. 40A-2-009.**  $\text{RbHSO}_4$ .  $\kappa'_c$  vs.  $T$  [84Pap]. Parameter:  $f$ . Up to 78.5 GHz.

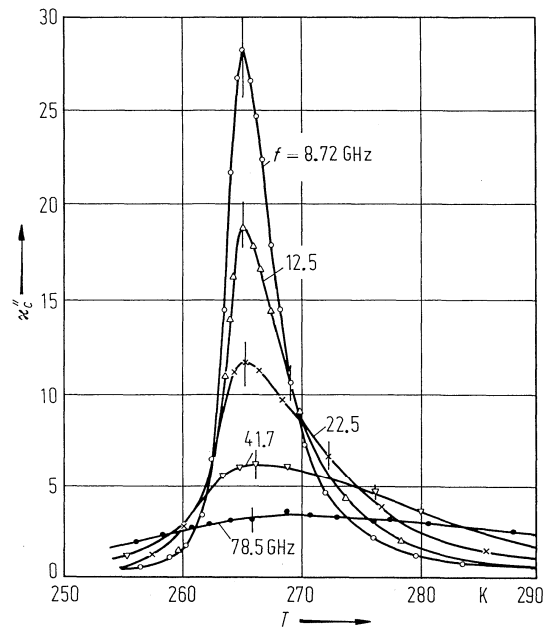


Fig. 40A-2-010.  $\text{RbHSO}_4$ .  $\kappa_c''$  vs.  $T$  [84Pap]. Parameter:  $f$ . Up to 78.5 GHz.

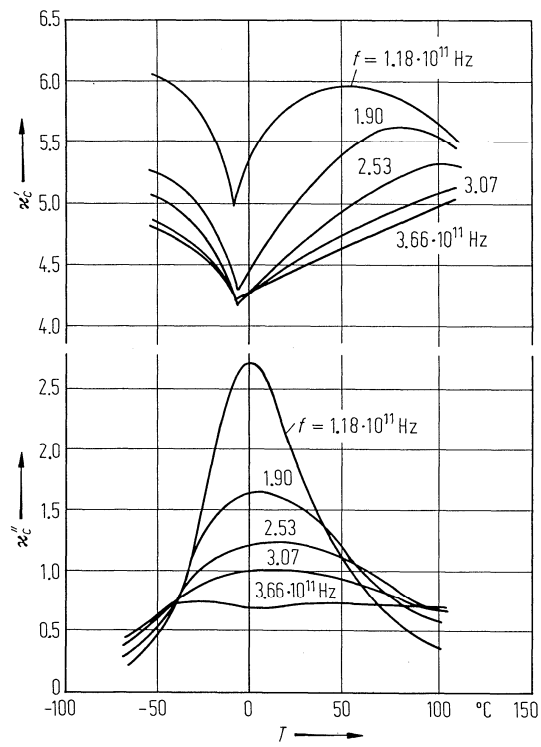
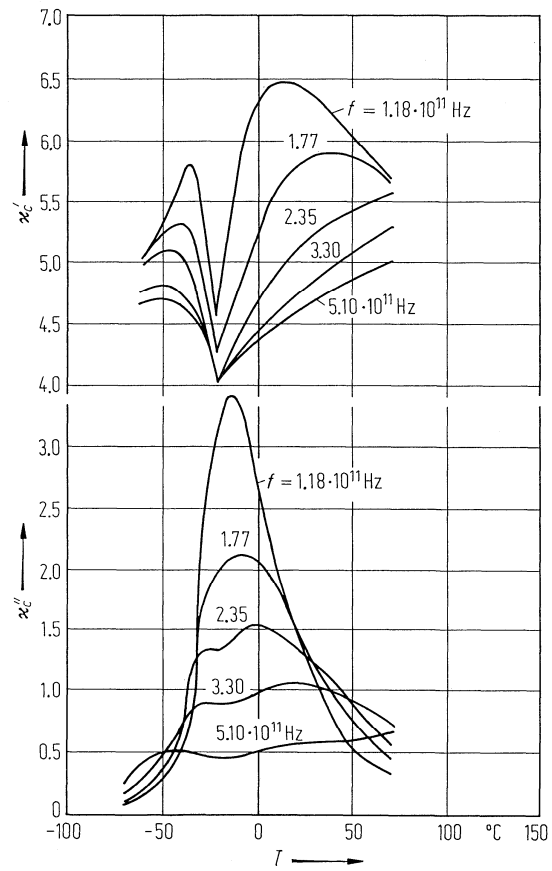
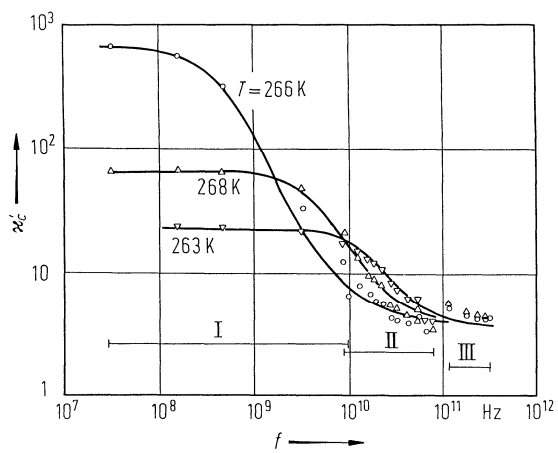


Fig. 40A-2-011.  $\text{RbHSO}_4$ .  $\kappa_c'$ ,  $\kappa_c''$  vs.  $T$  [83Amb]. Parameter:  $f$ . Up to 366 GHz.



**Fig. 40A-2-012.**  $\text{RbDSO}_4$ .  $\kappa'_c, \kappa''_c$  vs.  $T$  [83Amb]. Parameter:  $f$ . Up to 510 GHz.



**Fig. 40A-2-013.**  $\text{RbHSO}_4$ .  $\kappa'_c$  vs.  $f$  [85Gri]. Parameter:  $T$ . Data in the frequency range I were taken from [80Oza], III from [83Amb].

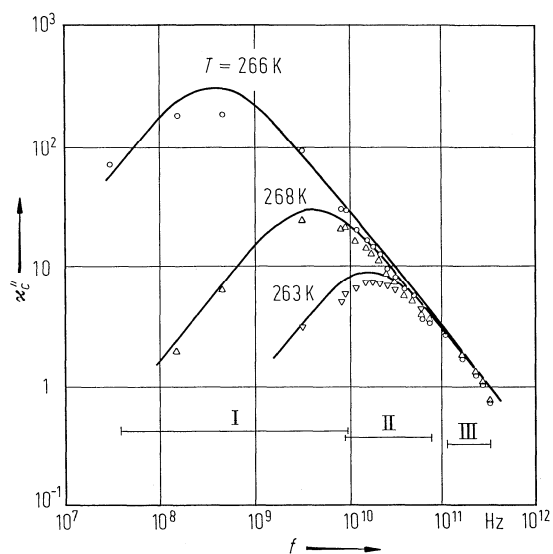


**Fig. 40A-2-014.**  $\text{RbHSO}_4$ .  $\kappa_c''$  vs.  $f$  [85Gri]. Parameter:  $T$ . Data in frequency range I were taken from [80Oza], III from [83Amb].

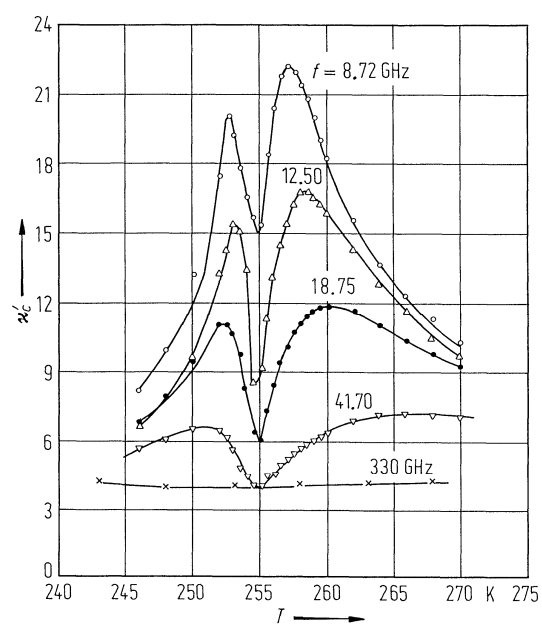


**Fig. 40A-2-015.**  $\text{RbH}_{0.3}\text{D}_{0.7}\text{SO}_4$ .  $\kappa_c'$  vs.  $T$  [84Gri]. Parameter:  $f$ . Up to 330 GHz.

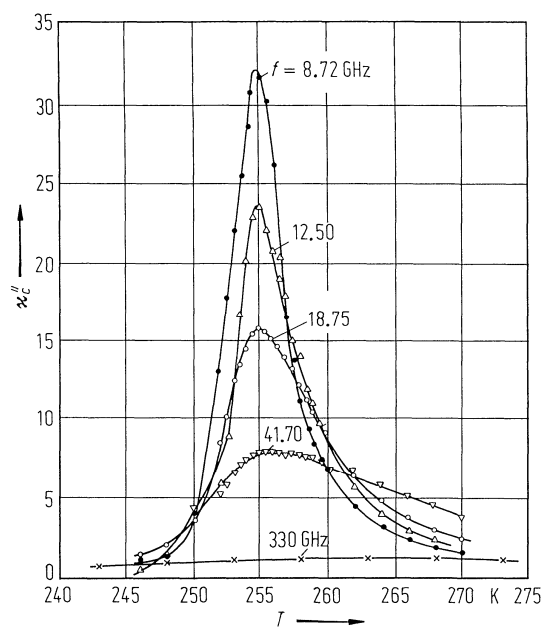


Fig. 40A-2-016.  $\text{RbH}_{0.3}\text{D}_{0.7}\text{SO}_4$ .  $\kappa_c''$  vs.  $T$  [84Gri]. Parameter:  $f$ . Up to 330 GHz.

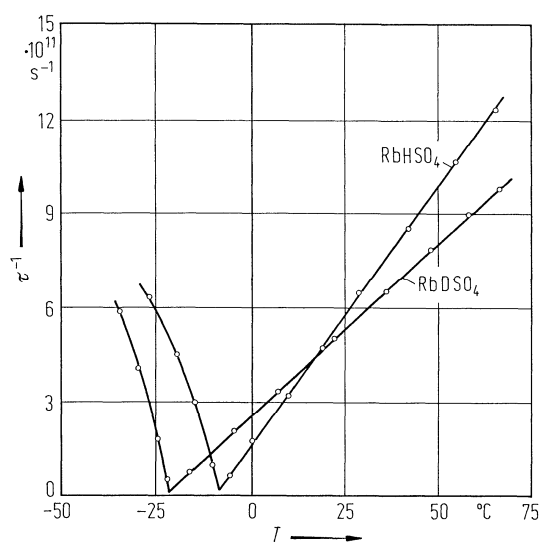


Fig. 40A-2-017.  $\text{RbHSO}_4$ ,  $\text{RbDSO}_4$ .  $\tau^{-1}$  vs.  $T$  [83Amb].  $\tau$ : dielectric relaxation time.



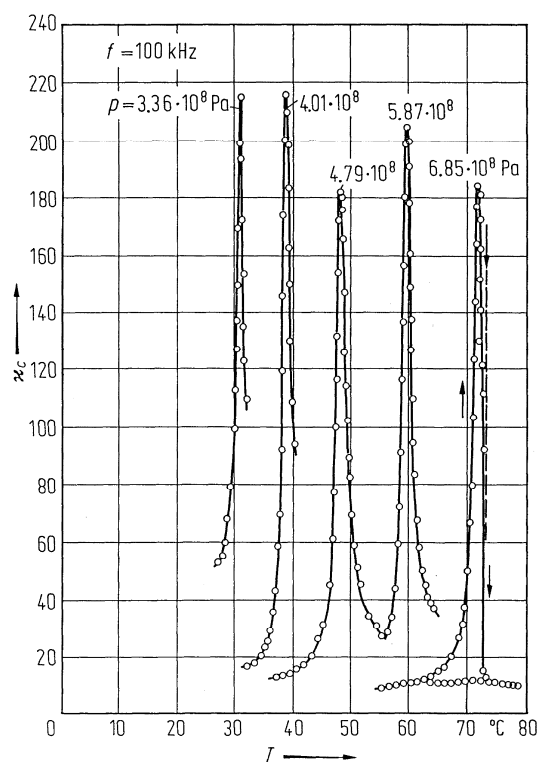


Fig. 40A-2-018.  $\text{RbHSO}_4$ .  $\kappa_c$  vs.  $T$  [75Ges]. Parameter:  $p$ .

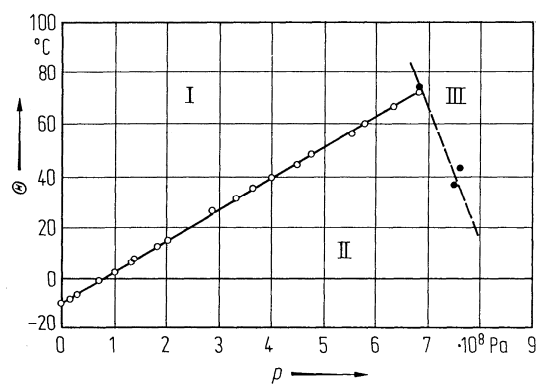
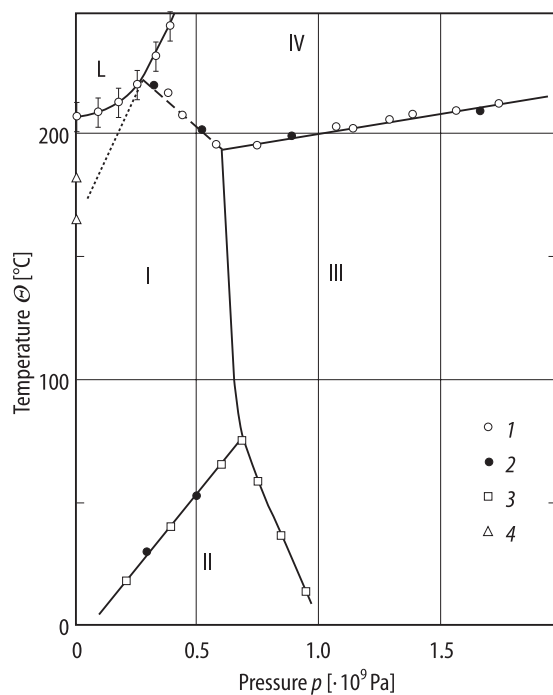
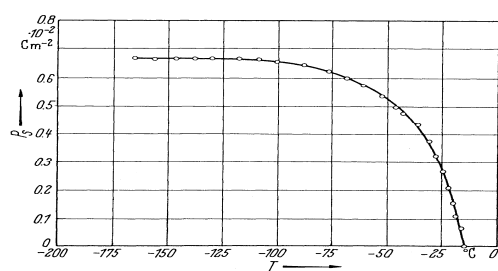


Fig. 40A-2-019.  $\text{RbHSO}_4$ .  $\Theta$  vs.  $p$  [75Ges].



**Fig. 40A-2-020.**  $\text{RbHSO}_4$ .  $\Theta$  vs.  $p$  [88Sin]. 1: DTA measurement, 2: electrical conductivity measurement, 3: data by [75Ges], 4: anomaly in surface conduction.



**Fig. 40A-2-021.**  $\text{RbHSO}_4$ .  $P_s$  vs.  $T$  [60Pep].

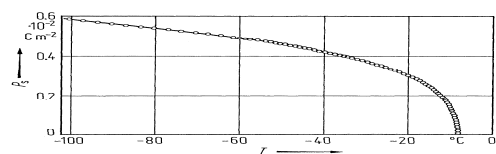


**Fig. 40A-2-022.**  $\text{RbHSO}_4$ .  $P_s$  vs.  $T$  [77Kaj].

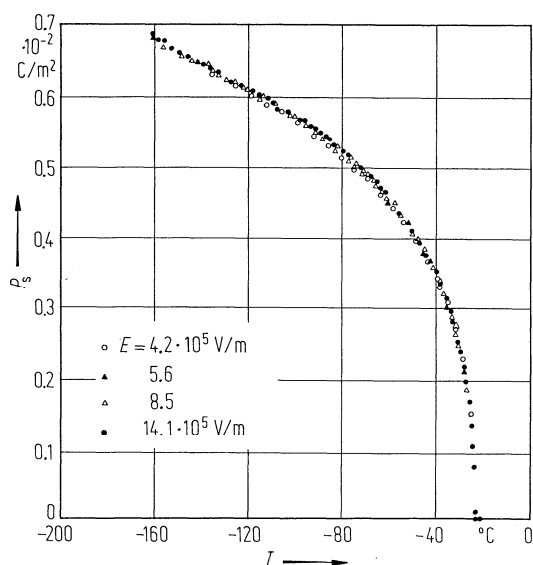


**Fig. 40A-2-023.**  $\text{RbDSO}_4$ .  $P_s$  vs.  $T$  [79Ich].  $E$ : maximum value of measuring field strength.

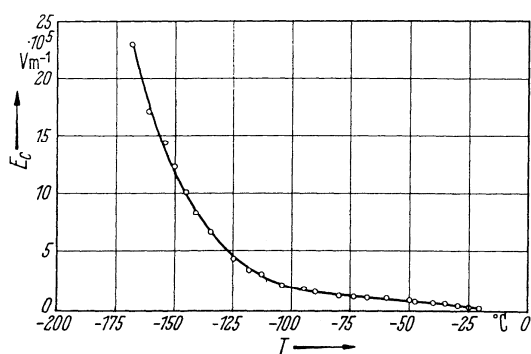


**Fig. 40A-2-024.**  $\text{RbHSO}_4$ .  $E_c$  vs.  $T$  [60Pep].

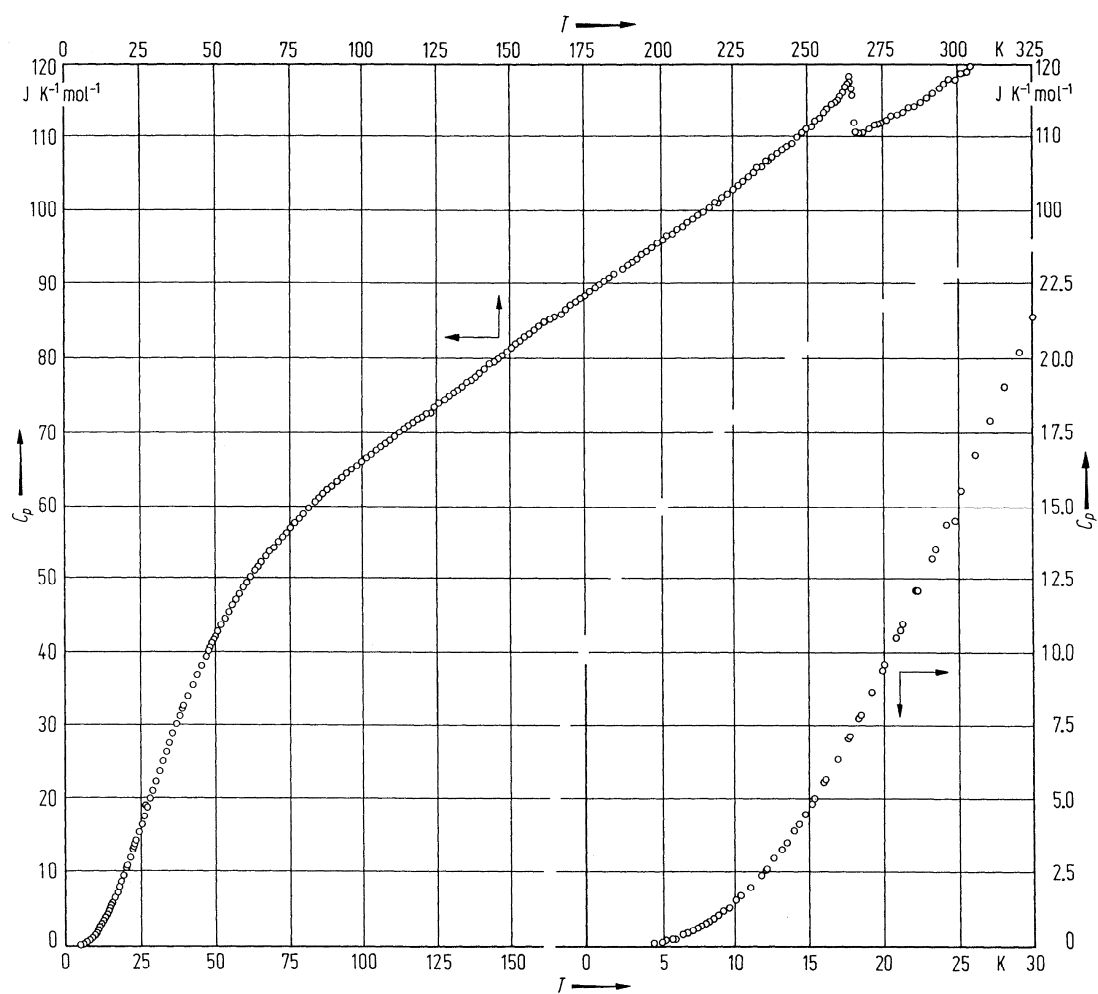
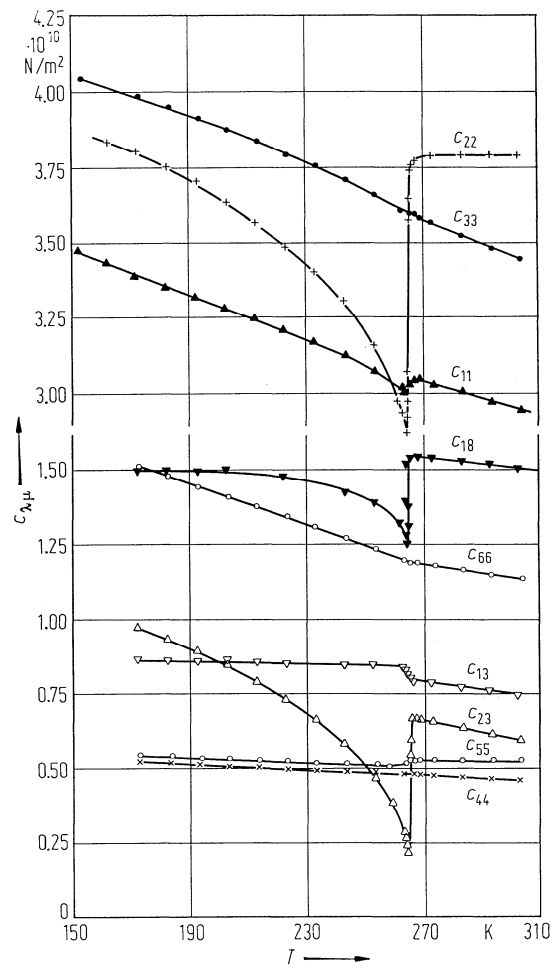
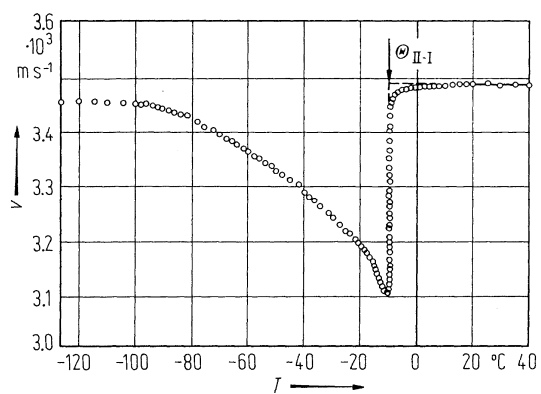


Fig. 40A-2-025.  $\text{RbHSO}_4$ .  $C_p$  vs.  $T$  [73Chi].



**Fig. 40A-2-026.**  $\text{RbHSO}_4$ .  $c_{\lambda\mu}$  vs.  $T$  [79Ich].  $c_{\lambda\mu}$ : elastic stiffness constant at  $f = 10 \text{ MHz}$ .



**Fig. 40A-2-027.**  $\text{RbHSO}_4$ .  $v$  vs.  $T$  [78Kaw].  $v$ : velocity of sound wave propagating along the  $b$  axis at  $5 \text{ MHz}$ .

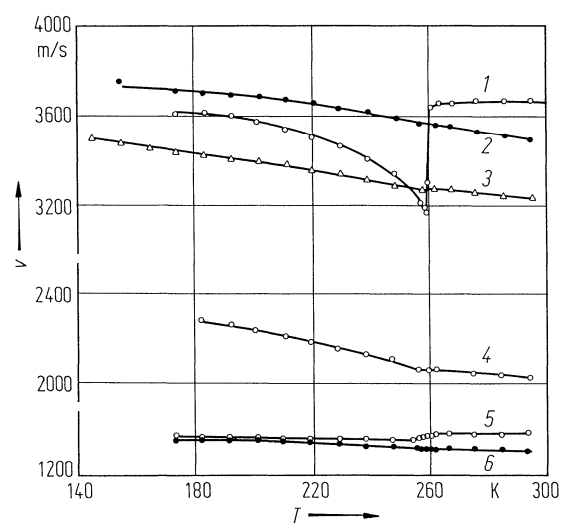


**Fig. 40A-2-028.**  $\text{RbHSO}_4$ .  $v$  vs.  $T$  [81Ale].  $v$ : ultrasonic velocity at 10 MHz. Curve 1: longitudinal,  $k \parallel [010]$ ; 2: longitudinal,  $k \parallel [001]$ ; 3: longitudinal,  $k \parallel [100]$ ; 4: shear,  $k \parallel [100]$ ,  $u \parallel [010]$ ; 5: shear,  $k \parallel [001]$ ,  $u \parallel [100]$ ; 6: shear,  $k \parallel [100]$ ,  $u \parallel [001]$ .

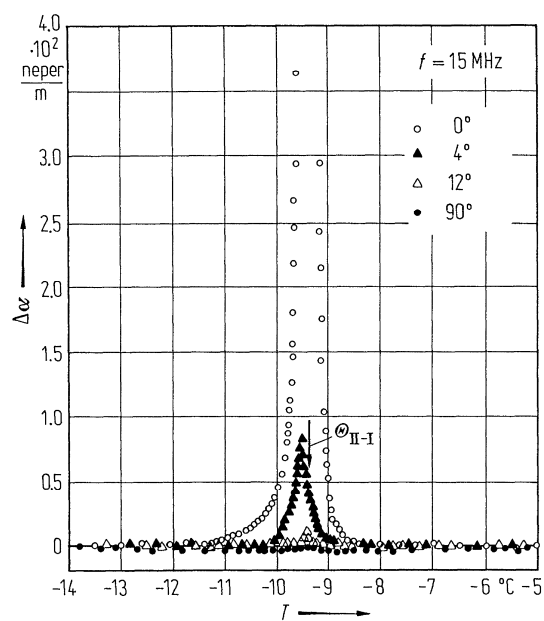


**Fig. 40A-2-029.**  $\text{RbHSO}_4$ .  $\Delta\alpha$  vs.  $T$  [78Kaw].  $\Delta\alpha$ : anomalous part of the attenuation of the quasi-longitudinal sound waves propagating along the direction in the  $bc$  plane with angles  $0^\circ$ ,  $4^\circ$ ,  $12^\circ$  and  $90^\circ$  with respect to the  $b$  axis.

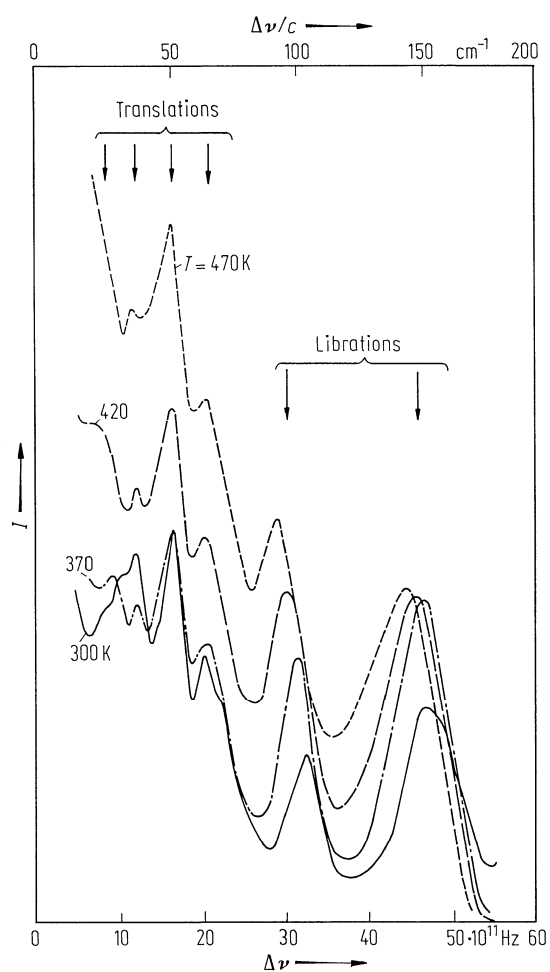


**Fig. 40A-2-030.**  $\text{RbHSO}_4$ .  $I$  vs.  $\Delta\nu$  [81Tou]. Parameter:  $T$ .  $I$ : Raman scattering intensity.  $\Delta\nu$ : Raman scattering frequency shift.

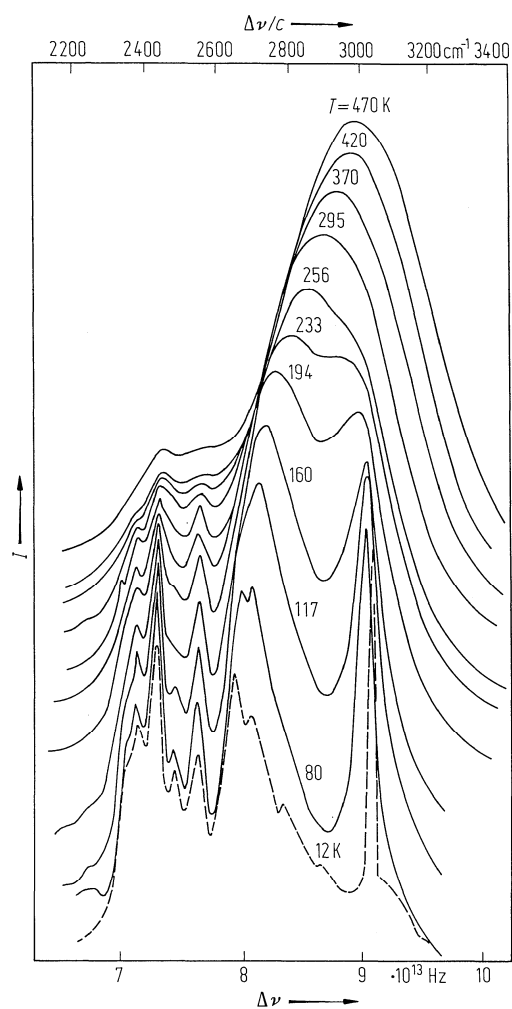


**Fig. 40A-2-031.**  $\text{RbHSO}_4$ .  $I$  vs.  $\Delta\nu$  [81Tou]. Parameter:  $T$ .  $I$ : Raman scattering intensity.  $\Delta\nu$ : Raman scattering frequency shift.



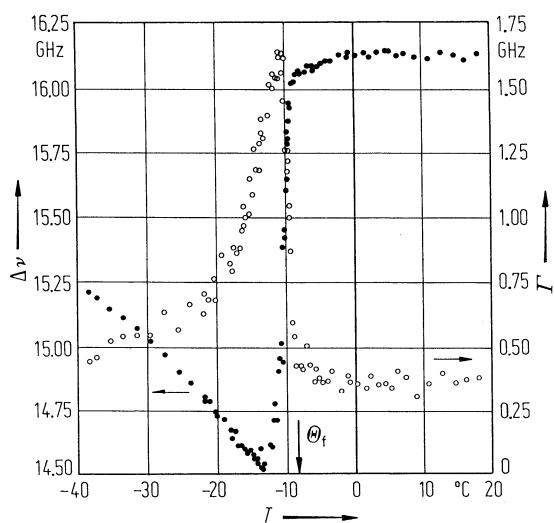


**Fig. 40A-2-032.**  $\text{RbHSO}_4$ .  $\Delta\nu$ ,  $\Gamma$  vs.  $T$  [81Tsu].  $\Delta\nu$ : Brillouin scattering frequency shift of the longitudinal acoustic phonon propagating along the  $b$  axis.  $\Gamma$ : full width at half maximum.  $\lambda = 488$  nm.  $90^\circ$  scattering.

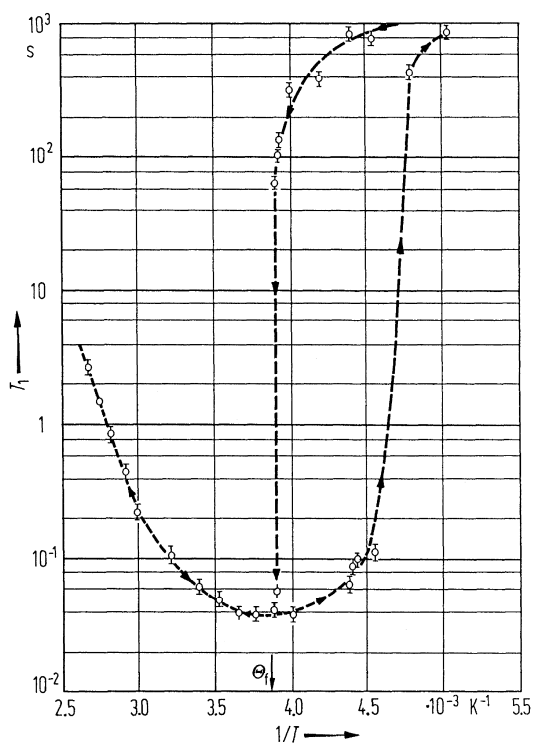


**Fig. 40A-2-033.**  $\text{RbHSO}_4$ .  $T_1$  vs.  $1/T$  [69Sil].  $T_1$ : spin-lattice relaxation time of  $^1\text{H}$ .